Inorg. Chem. **1994**, *33*, 3028–3031

Articles

Hydrothermal Synthesis and Crystal Structures of $NaCo_3(PO_4)(HPO_4)_2$ and $NaCo_3(AsO_4)(HAsO_4)_2$: Synthetic Modifications of the Mineral Alluaudite

Kwang-Hwa Lii* and Pei-Fen Shih

Institute of Chemistry, Academia Sinica, Taipei, Taiwan, ROC

Received December 7, 1993⊗

Two cobalt-containing analogues of the mineral alluaudite, $NaCo_3(XO_4)(HXO_4)_2$ (X = P, As), have been synthesized by hydrothermal methods and characterized by single-crystal X-ray diffraction. Crystal data: $NaCo_3(PO_4)(HPO_4)_2$, monoclinic, $C2/c$, $a = 11.865(2)$ Å, $b = 12.137(2)$ Å, $c = 6.512(1)$ Å, $\beta = 114.12(1)°$, $V = 855.9(2)$ Å^3, $Z = 4$, $R = 0.0373$; $NaCo_3(AsO_4)(HAsO_4)_2$, as above except $a = 12.054(1)$ Å, $b = 12.378(1)$ Å, $c = 6.780(2)$ Å, $\beta = 113.03(1)°$, $V = 931.0(3)$ Å^3, $R = 0.0177$. The two compounds are isostructural. The framework consists of parallel infinite chains of CoO_6 octahedra sharing their skew edges, which are linked by XO_4 and HXO_4 groups to form a three-dimensional architecture with two types of channels running along the c-axis. Sodium ions are located in sites within one channel with the other channel being occupied by OH groups. The structure is compared with that of a natural alluaudite. Magnetic susceptibility measurements on a powder sample of $NaCo_3(PO_4)(HPO_4)_2$ were performed.

Introduction

The phosphates of the alluaudite series of minerals have compositions in the range from $X(2)^{+}X(1)^{+}M(1)^{2+}M(2)_2^{2+}(PO_4)_3$ to $X(1)^{+}M(1)^{2+}M(2)_2^{3+}(PO_4)_3$.[1,2] For the unoxidized end member, $X(2)^{+}X(1)^{2+}M(1)^{2+}M(2)_2^{2+}(PO_4)_3$, X(1) is predominantly Ca^{2+}, $X(2) = Na^{+}$, $M(1) = Mn^{2+}$, and $M(2) = Fe^{2+}$, resulting in a composition for $Z = 4$ of $NaCaMn^{2+}Fe_2^{2+}(PO_4)_3$. The structure appears to be highly susceptible to partial oxidation, since no unoxidized end-member compositions are known. One the other hand, the oxidized end member, $NaMn^{2+}Fe_2^{3+}(PO_4)_3$, does not proceed to the completely oxidized equivalent $Mn^{3+}Fe_2^{3+}(PO_4)_3$. Most natural samples involve mixed Fe valences and are derivatives of the composition $NaNaMn^{2+}(Fe^{2+}Fe^{3+})(PO_4)_3$. The crystal structure of alluaudite consists of parallel chains of edge-sharing M(1)–O and M(2)–O polyhedra, which are linked by phosphate tetrahedra to form sheets. Symmetry-equivalent sheets are held together by phosphate oxygens to form a three-dimensional architecture with channels parallel to the c-axis which are filled by X(1) and X(2) cations. The mineral caryinite, an arsenate containing Mn, Mg, Ca, Pb, and Na, has been suggested to belong to the alluaudite structure type.[2-4] To our knowledge, the crystal structure of caryinite has not yet been reported.

In nature many minerals crystallize from hot, water-rich solutions. By using autoclaves, hydrothermal growth in the laboratory closely duplicates the natural process. For examples, crystals of leucophosphite, $KFe_2(PO_4)_2(OH)(H_2O)\cdot H_2O$,[5] and a triclinic polymorph of sincosite, $Ca(VO)_2(PO_4)_2\cdot 4H_2O$,[6] have been synthesized hydrothermally in our laboratory. In this work we reported the synthesis and crystal structures of $NaCo_3(PO_4)(HPO_4)_2$ and $NaCo_3(AsO_4)(HAsO_4)_2$, two pure cobalt-containing analogues of the mineral alluaudite.

Experimental Section

Synthesis. Reagent grade chemicals were used as received. A purple crystalline product was prepared by hydrothermal reaction of $NaH_2PO_4\cdot 2H_2O$ (0.753 g), $Co(OH)_2$ (0.448 g), H_3PO_4 (0.32 mL, 85%) (molar ratio Na:Co:P = 1:1:2), and water (12 mL) in a Teflon-lined autoclave (23 mL) at 230 °C for 4 d followed by slow cooling to room temperature at 5 °C/h. The product was filtered off, washed with water, rinsed with ethanol, and dried in a desiccator at ambient temperature. The product contained purple rod-shaped crystals of $NaCo_3(PO_4)(HPO_4)_2$. Its bulk X-ray powder pattern, obtained by using a MAC Science MXP18 powder diffractometer, compared very well with that calculated from the single-crystal data. A TG analysis under N_2 showed an one-step weight loss of 4.2% at ca. 500 °C. The value is somewhat higher than that expected from a structural formula of $NaCo_3(PO_4)(HPO_4)_2$ (3.7%). Energy-dispersive X-ray fluorescence (EDX) analysis on a purple crystal showed that the Na:Co:P mole ratio was 0.99:3:3.02.

The crystal growth of $NaCo_3(AsO_4)(HAsO_4)_2$ was achieved by heating a reaction mixture of $Na_2HAsO_4\cdot 7H_2O$ (1.095 g), $Co(OH)_2$ (0.326 g), H_3AsO_4 (1.82 g, 80%) (molar ratio Na:Co:As = 1:1:3), and water (7 mL) at 400 °C in a gold-lined Morey-type closure autoclave (5.2 cm × 2 cm inside diameter) with an internal volume of 16 cm^3 for 2 d and then cooled to room temperature in 8 h. The product contained purple crystals of $NaCo_3(AsO_4)(HAsO_4)_2$. Powder X-ray diffraction of the bulk product indicated that a single-phase product was also obtained. EDX analysis on a purple crystal showed that the Na:Co:As mole ratio was 1.06:3:3.06. Reactions at 230 °C yielded polycrystalline product only.

Crystallographic Analysis. Two crystals of dimensions 0.05 × 0.05 × 0.15 mm for $NaCo_3(PO_4)(HPO_4)_2$ (**1**) and 0.04 × 0.06 × 0.31 mm for $NaCo_3(AsO_4)(HAsO_4)_2$ (**2**) were selected for indexing and intensity data collection on an Enraf-Nonius CAD4 diffractometer with κ geometry using graphite-monochromated Mo Kα radiation. Axial oscillation photographs were taken to check the unit cell parameters and symmetry properties. Octants collected: $\pm h,+k,+l$ for compound **1**; $+h,+k,\pm l$ for compound **2**. 2θ range: 2–55° for both compounds. Of the 1074 (1116) reflections collected 703 (972) unique reflections were considered observed ($I > 2.5\sigma(I)$) after Lorentz polarization and empirical absorption corrections for compounds **1**, and **2**, respectively. Correction for absorption was based on ψ scans of a few suitable reflections with χ values close to 90° using the NRC VAX program package.[7] $T_{min/max} = 0.759/1.0$ and 0.694/1.0 for **1** and **2**, respectively. On the basis of the systematic absences,

---

* To whom correspondence should be addressed.

⊗ Abstract published in *Advance ACS Abstracts*, June 1, 1994.

(1) Fisher, D. J. *Am. Mineral.* **1955**, *40*, 1100.

(2) Moore, P. B. *Am. Mineral* **1971**, *56*, 1955.

(3) Bostrom, K. *Ark. Mineral. Geol.* **1957**, *2*, 333.

(4) Strunz, H. *Neues Jahrb. Mineral. Monatsh.* **1960**, 7.

(5) Wu, L.-S.; Lii, K.-H. Unpublished research.

(6) Kang, H.-Y.; Lee, W.-C.; Wang, S.-L.; Lii, K.-H. *Inorg. Chem.* **1992**, *31*, 4743.

(7) Gabe, E. J.; Le Page, Y.; Charland, J. P.; Lee, F. L. *J. Appl. Crystallogr.* **1989**, *22*, 384.

0020-1669/94/1333-3028$04.50/0

Table 1. Crystallographic Data for $NaCo_3(PO_4)(HPO_4)_2$ (**1**) and $NaCo_3(AsO_4)(HAsO_4)_2$ (**2**)

	1	**2**
formula	$Co_3H_2NaO_{12}P_3$	$As_3Co_3H_2NaO_{12}$
fw	486.71	618.56
space group	*C*2/*c* (No. 15)	*C*2/*c* (No. 15)
a, Å	11.865(2)	12.054(1)
b, Å	12.137(2)	12.378(1)
c, Å	6.512(1)	6.780(2)
β, deg	114.12(1)	113.03(1)
V, Å^3	855.9(2)	931.0(3)
Z	4	4
μ(Mo Kα), cm^{-1}	64.3	159.8
ρ_{calcd}, g·cm^{-3}	3.777	4.413
λ, Å	0.709 30	0.709 30
T, °C	23	23
R^a	0.0373	0.0177
R_w^{b}	0.0399	0.0208

[a] $R = \sum||F_o| - |F_c||/\sum|F_o|$. [b] $R_w = [\sum w(|F_o| - |F_c|)^2/\sum w|F_o|^2]^{1/2}$, $w = [\sigma^2(F) + gF^2]^{-1}$.

Table 2. Atomic Coordinates and Thermal Parameters (Å^2 × 100) for $NaCo_3(PO_4)(HPO_4)_2$ (**1**) and $NaCo_3(AsO_4)(HAsO_4)_2$ (**2**)

	x	*y*	*z*	U_{eq}^{a}
		Compound **1**		
Na	0	0.0246(5)	0.75	3.9(2)
Co(1)	0	0.2810(1)	0.25	1.03(4)
Co(2)	0.29008(8)	0.66232(8)	0.3758(1)	0.89(3)
P(1)	0	−0.3158(2)	0.25	0.80(7)
P(2)	0.2183(1)	−0.1114(1)	0.1125(3)	0.77(5)
O(1)	0.4647(4)	0.7432(4)	0.5394(7)	1.1(1)
O(2)	0.1074(4)	0.6077(4)	0.2645(7)	1.1(1)
O(3)	0.3463(4)	0.6719(4)	0.1127(7)	1.0(1)
O(4)	0.1415(4)	0.4080(4)	0.3430(7)	1.1(1)
O(5)	0.2151(4)	0.8207(4)	0.3067(7)	0.9(1)
O(6)	0.3443(4)	0.4990(4)	0.4004(7)	1.1(1)
H^b	0.8766	0.4831	0.1775	5
		Compound **2**		
Na	0	0.0040(2)	0.75	3.05(9)
Co(1)	0	0.28195(5)	0.25	0.86(2)
Co(2)	0.29406(4)	0.66026(4)	0.38280(7)	0.74(2)
As(1)	0	−0.31074(4)	0.25	0.72(2)
As(2)	0.22017(3)	−0.11511(3)	0.11316(5)	0.64(1)
O(1)	0.4662(2)	0.7365(2)	0.5269(3)	0.90(7)
O(2)	0.1149(2)	0.6049(2)	0.2696(4)	1.08(8)
O(3)	0.3471(2)	0.6775(2)	0.1255(4)	0.90(7)
O(4)	0.1307(2)	0.4070(2)	0.3350(4)	1.12(8)
O(5)	0.2126(2)	0.8116(2)	0.3152(4)	0.84(7)
O(6)	0.3513(2)	0.5029(2)	0.4022(4)	0.92(8)
H^b	0.8808	0.4884	0.1986	5

[a] U_{eq} is defined as one-third of the trace of the orthogonalized U_{ij} tensor. [b] The atomic coordinates and thermal parameters for the H atoms are fixed.

Table 3. Bond Lengths (Å) and Bond Valence Sums ($\sum$s) for $NaCo_3(PO_4)(HPO_4)_2$ (**1**) and $NaCo_3(AsO_4)(HAsO_4)_2$ (**2**)

Compound **1**			
$\sum$s(Na–O) = 1.15			
Na–O(1)	2.937(7) (2×)	Na–O(3)	2.912(7) (2×)
Na–O(5)	3.067(6) (2×)	Na–O(6)	2.293(4) (2×)
Na–O(6)	2.436(6) (2×)		
$\sum$s(Co(1)–O) = 1.74			
Co(1)–O(1)	2.141(5) (2×)	Co(1)–O(3)	2.132(4) (2×)
Co(1)–O(4)	2.175(4) (2×)		
$\sum$s(Co(2)–O) = 2.02			
Co(2)–O(1)	2.142(4)	Co(2)–O(2)	2.092(4)
Co(2)–O(3)	2.081(6)	Co(2)–O(5)	2.088(4)
Co(2)–O(5)	2.103(5)	Co(2)–O(6)	2.070(5)
$\sum$s(P(1)–O) = 4.89			
P(1)–O(1)	1.537(5) (2×)	P(1)–O(2)	1.548(5) (2×)
$\sum$s(P(2)–O) = 4.93			
P(2)–O(3)	1.536(5)	P(2)–O(4)	1.585(5)
P(2)–O(5)	1.523(5)	P(2)–O(6)	1.517(5)
H–O(4)	0.934	H···O(2)	1.552
Compound **2**			
$\sum$s(Na–O) = 1.00			
Na–O(3)	2.818(3) (2×)	Na–O(6)	2.338(2) (2×)
Na–O(6)	2.395(3) (2×)		
$\sum$s(Co(1)–O) = 1.82			
Co(1)–O(1)	2.146(3) (2×)	Co(1)–O(3)	2.136(2) (2×)
Co(1)–O(4)	2.121(2) (2×)		
$\sum$s(Co(2)–O) = 2.02			
Co(2)–O(1)	2.136(2)	Co(2)–O(2)	2.104(2)
Co(2)–O(3)	2.090(3)	Co(2)–O(5)	2.081(2)
Co(2)–O(5)	2.110(3)	Co(2)–O(6)	2.053(2)
$\sum$s(As(1)–O) = 4.95			
As(1)–O(1)	1.678(2) (2×)	As(1)–O(2)	1.698(3) (2×)
$\sum$s(As(2)–O) = 4.95			
As(2)–O(3)	1.687(2)	As(2)–O(4)	1.713(3)
As(2)–O(5)	1.675(3)	As(2)–O(6)	1.678(2)
H–O(4)	1.030	H···O(2)	1.456

statistics of intensity distribution, and successful solution and refinement of the structures, the space groups for both compounds were determined to be *C*2/*c*. Direct methods were used to locate the metal atoms with the remaining non-hydrogen atoms being found from successive difference maps. On the basis of bond-length bond-strength calculations,[8] cobalt atoms are divalent, O(2) and O(4) in both structures were considerably undersaturated, and all other oxygen atoms had valence sums close to 2.0. Valence sums of 1.54 and 1.36 vu (vu = valence unit) were calculated for O(2) and O(4) in **1** and 1.53 and 1.47 vu in **2**. In order to balance the charge, one hydrogen atom must be included in the formula. The O(2)–O(4) distances (between O's of different XO_4^{3-} ions) having values of 2.477 Å in **1** and 2.483 Å in **2** indicate strong hydrogen bonding. The values of the valence sums of O(2) and O(4) also suggest that they are bonded to a common hydrogen atom. The hydrogen atom was located from a difference electron density map which was calculated by using structure factors obtained from intensity data with $2\theta < 40°$. The multiplicities of Na and Co atoms were refined but did not deviate significantly from full occupancy. The final cycles of refinement, including the atomic coordinates and anisotropic thermal parameters for all non-hydrogen atoms and a fixed isotropic thermal parameter for the H atom, converged at $R = 0.0375$ and $R_w = 0.0401$ for **1** and $R = 0.0177$ and $R_w = 0.0208$ for **2**. In the final difference electron density map the deepest hole was −0.65 e/Å^3 (−0.52 e/Å^3) and the highest peak 1.09 e/Å^3 (0.53 e/Å^3) for **1** and **2**, respectively. The atom labeling is the same as that for a mineral alluaudite[2] in order to make comparisons. Neutral-atom scattering factors for all atoms were used.[9] Anomalous dispersion and secondary extinction corrections were applied. Structure solution and refinement were performed on a DEC MicroVAX computer system using SHELXTL-Plus programs.[10]

Magnetic Susceptibility. In order to help assign the oxidation state of the Co atoms, magnetization data were obtained on 262.69 mg of powder $NaCo_3(PO_4)(HPO_4)_2$ from 2 to 300 K in a magnetic field of 5 kG after zero-field cooling using a SQUID magnetometer. Observed susceptibilities were corrected for diamagnetism according to Selwood.[11]

Results and Discussion

The crystallographic data are listed in Table 1, atomic coordinates and thermal parameters in Table 2, and selected bond distances and bond valence sums[8] in Table 3. Bond valence sums for the Na, Co(2), P, and As atoms are in good accordance with their formal oxidation states. The value for Co(1) is somewhat lower. In the following, only the structure of $NaCo_3(PO_4)(HPO_4)_2$ will be discussed because the two compounds are isostructural.

The framework of $NaCo_3(PO_4)(HPO_4)_2$ consists of infinite chains of CoO_6 octahedra sharing skew edges running parallel

---

(8) Brown, I. D.; Altermatt, D. *Acta Crystallogr.* **1985**, *B41*, 244.

(9) *International Tables for X-Ray Crystallography*; Kynoch Press: Birmingham, England, 1974; Vol. IV.

(10) Sheldrick, G. M. *SHELXTL-PLUS Crystallographic System, Release 4.11*; Siemens Analytical X-Ray Instruments, Inc.: Madison, WI, 1990.

(11) Selwood, P. W. *Magnetochemistry*; Interscience: New York, 1956.

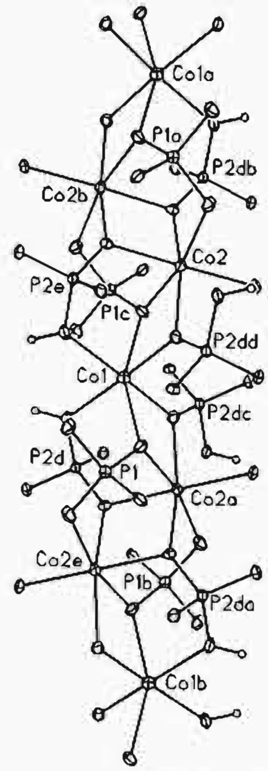

Figure 1. View of a section of an infinite chain showing the coordination of phosphate ligands around CoO_6 octahedra in $NaCo_3(PO_4)(HPO_4)_2$. Thermal ellipsoids are shown at 60% probability.

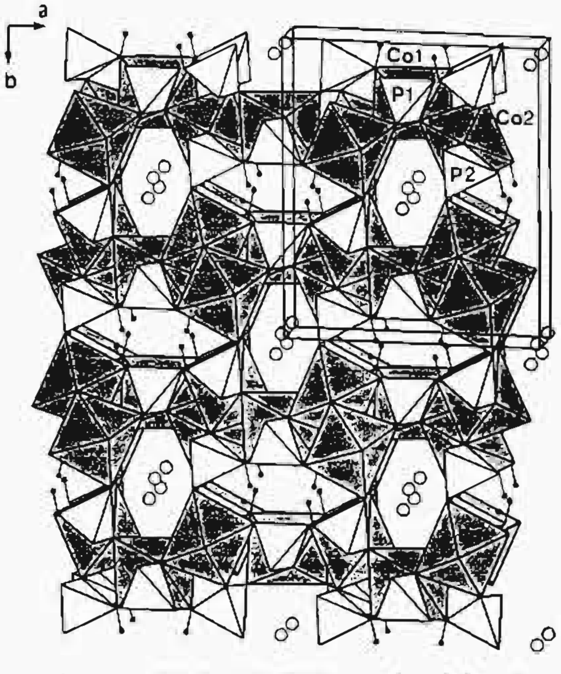

Figure 2. Structure of $NaCo_3(PO_4)(HPO_4)_2$ as viewed along the *c*-axis. In this presentation, the corners of octahedra and tetrahedra are oxygen atoms and the cobalt and phosphorus are at the center of each octahedron and tetrahedron, respectively. Large open and small solid circles are sodium and hydrogen atoms, respectively.

to the [101] direction (Figure 1). These infinite chains are linked by PO_4 and HPO_4 groups to form sheets parallel to (010). Adjacent sheets, which are related by 2_1-screw axis operation, are connected by HPO_4 groups such that an open-framework network, with two sets of channels along the *c*-axis is formed (Figure 2). The sodium ions lie within one of the two sets of channels. The OH groups point into the second set of channels.

Atoms Na, Co(1), and P(1) (or As(1)) sit on 2-fold axes, and

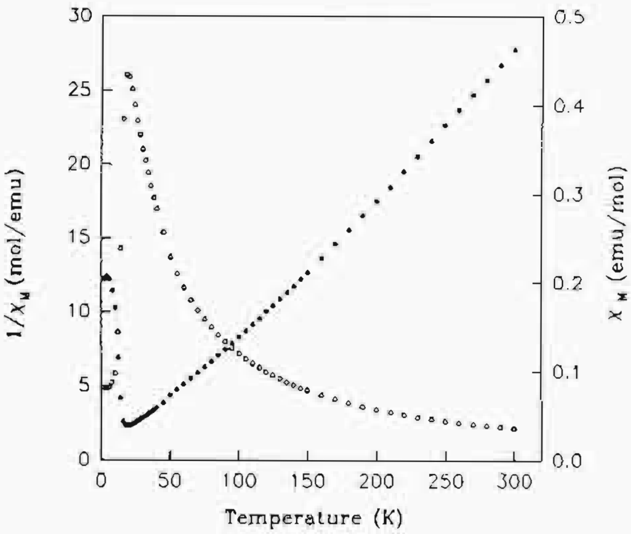

Figure 3. Magnetic susceptibility (χ_M, open circles) and inverse magnetic susceptibility ($1/\chi_M$, solid circles) plotted as a function of temperature for a powder sample of $NaCo_3(PO_4)(HPO_4)_2$.

all other atoms are at general positions. The coordination numbers of the sodium ions were determined on the basis of the maximum gap in the Na–O distances ranked in increasing distances. The maximum cation–anion distance, L_{max}, according to Donnay and Allmann was also considered.[12] The L_{max} for Na–O is 3.13 Å. The sodium ion in $NaCo_3(PO_4)(HPO_4)_2$ is bound to four oxygen atoms at distances of 2.293 Å (2×) and 2.436 Å (2×) and six others at distances ranging from 2.912 from 3.067 Å. The sodium ion in $NaCo_3(AsO_4)(HAsO_4)_2$ is coordinated by six oxygens at distances from 2.338 to 2.818 Å and interacting with four others at 3.202 Å (2×) and 3.330 Å (2×).

Atom Co(1) sits on a 2-fold axis and has a more symmetric neighborhood than Co(2). Each $Co(1)O_6$ octahedron shares skew edges with two $Co(2)O_6$, and each $Co(2)O_6$ shares skew edges with one $Co(1)O_6$ and one $Co(2)O_6$. The midpoint of the shared edge of Co(2)–O octahedral pair is an inversion center. The oxygen atoms forming the shared edges are also shared by $P(1)O_4$ or $HP(2)O_4$ groups. Octahedra within a chain are linked by two oxygen atoms of PO_4 with the remaining two oxygens linking to adjacent chains in the same sheet. The HPO_4 group links two oxygen atoms to octahedra within a chain, one to an adjacent chain in the same sheet and the remaining oxygen to an adjacent sheet. As shown by the O–O distances 2.693–3.497 Å for $Co(1)O_6$ and 2.693–3.452 Å for $Co(2)O_6$, and the cis O–Co–O bond angles 78.2–108.3° for $Co(1)O_6$ and 79.2–111.6° for $Co(2)O_6$, both octahedra are strongly distorted. The great spread of the O–Co–O bond angles and O–O edges is mainly caused by various kinds of polyhedral connections. The Co–O bond length distortion is small, and the elongation of CoO_6 octahedra along one 4-fold axis is unclear. This is expected because Jahn–Teller distortion in the high-spin d^7 configuration is considerably weaker than for the configurations involving splitting of the e_g level. The average Co(1)–O bond length (2.149 Å) is greater than the mean value of 2.111 Å derived from 672 Co–O bonds by Wildner,[13] but the average Co(2)–O bond length (2.096 Å) is smaller. The Co–O bond length distortion in $Co(1)O_6$ is to the same extent as that in $Co(2)O_6$. In contrast crystal structure analysis of a natural alluaudite from the Buranga pegmatite of Central Africa indicates that the M–O bond length distortion in $M(2)O_6$ is considerably more pronounced than that in $M(1)O_6$.[2] The common edge of $Co(1)O_6$ and $Co(2)O_6$ is the shortest (2.693 Å). The edge shared by two $Co(2)O_6$ is longer (2.875 Å). Atoms O(5), which form the longer shared edge, are each shared by a HPO_4 group which

---

(12) Donnay, G.; Allman, R. *Am. Mineral.* **1970**, *55*, 1003.
(13) Wildner, M. *Z. Kristallogr.* **1992**, *202*, 51.

also bridges over adjacent Co(1) and Co(2) within the same chain, and consequently O(5)'s are restrained from approaching to each other. The shortening of shared edges is evidence that the structure is predominantly ionic.

Figure 3 shows the magnetic susceptibility and inverse magnetic susceptibility of $NaCo_3(PO_4)(HPO_4)_2$ plotted as a function of temperature. At higher temperatures (50–300 K), $\chi_M T$ remains essentially constant (ca. 11–12 emu·K/mol). At lower temperatures the magnetic susceptibility rises sharply to a maximum at ca. 25 K and then decreases just as sharply. This behavior should be due to antiferromagnetic ordering of Co ions. The data above 150 K were least-squares fitted to a Curie–Weiss equation: $\chi_M = C/(T - \Theta)$ where $C = 9.85$ cm^3·K/mol and $\Theta = 26$ K. From the relation $C = N\mu_{\mathrm{eff}}^2/3k_B$ one obtains the effective magnetic moment μ_{eff} per metal atom = 5.13 μ_B, which is considerably higher than the spin-only value of 3.87 μ_B. The effective magnetic moments for Co(II) complexes around room temperature are between 4.7 and 5.2 μ_B because of orbital contribution. The magnetic susceptibility alone does not exclude the presence of Co(III) ions because octahedral complexes with the d^6 configuration typically have a moment of 5.1–5.7 μ_B. However, the purple color of the crystal is indicative of the absence of mixed-valence states of cobalt in the crystal. The bond-length bond-strength calculation and TG analysis results strongly support the pressure of the H atom.

To our knowledge, the pure cobalt-containing form of the mineral alluaudite is observed for the first time. The structure has two sets of infinite channels parallel to the *c*-axis. One channel is located at $^1/_2, 0, z$ (X1), and the other one, at $0, 0, z$ (X2). The Na^+ ions are located in channel X2, and OH groups point into X1. The coordination polyhedron of Na^+ is highly irregular and consists of an inner coordination shell of four oxygen atoms and an outer shell of six oxygens (Figure 4). In contrast, in Buranga alluaudite channel X2 is empty but X1 is partly filled with Na^+, Ca^{2+}, and Mn^{2+}. The X1 site in the Buranga sample is coordinated by eight oxygen atoms defining a cube. In the pure iron-containing compound $NaFe_3P_3O_{12}$,[14] which is also a synthetic modification of alluaudite, channel X2 is occupied by Na^+ and X1 is empty. To balance charge, iron atoms at the M(2) site are oxidized to 3+. Since the oxidation of Co^{2+} to Co^{3+} appears less favorable, an alternative to balance charge is to receive a proton by each $P(2)O_4$ as observed in the title compounds.

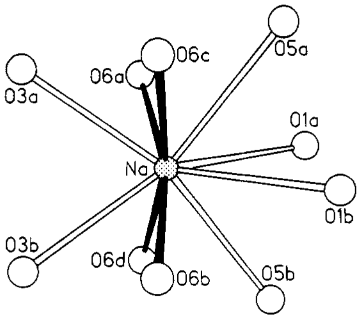

Figure 4. The coordination environment of the Na^+ ion in $NaCo_3(PO_4)(HPO_4)_2$ viewed in a direction approximately parallel to the *c*-axis. The solid and open full lines are short (2.293–2.436 Å) and long (2.912–3.067 Å) bonds, respectively.

Acknowledgment. We wish to acknowledge the Institute of Chemistry, Academia Sinica, and the National Science Council for financial support.

Supplementary Material Available: Tables giving crystal data and details of the structure determination, anisotropic thermal parameters, and bond lengths and angles (7 pages). Ordering information is given on any current masthead page.

---

(14) Corbin, D. R.; Whitney, J. F.; Fultz, W. C.; Stucky, G. D.; Eddy, M. M.; Cheetham, A. K. *Inorg. Chem.* **1986**, *25*, 2279.